Journal of Zhejiang University-SCIENCE A (Applied Physics & Engineering) 2025 26(5):492-498
www.jzus.zju.edu.cn; www.springer.com/journal/11582
E-mail: jzus_a@zju.edu.cn

Correspondence

https://doi.org/10.1631/jzus.A2400062

Check for updates

COM trajectory planning and disturbance-resistant control of a bipedal robot based on CP-ZMP-COM dynamics

Chunbiao GAN[1,2]✉, Zijing LI[1,2], Yimin GE[1,2], Mengyue LU[1,2]

[1]*State Key Laboratory of Fluid Power and Mechatronic Systems, School of Mechanical Engineering, Zhejiang University, Hangzhou 310058, China*

[2]*Key Laboratory of Advanced Manufacturing Technology of Zhejiang Province, School of Mechanical Engineering, Zhejiang University, Hangzhou 310058, China*

1 Introduction

To date, in model-based gait-planning methods, the dynamics of the center of mass (COM) of bipedal robots have been analyzed by establishing their linear inverted pendulum model (LIPM) or extended forms (Owaki et al., 2010; Englsberger et al., 2015; Xie et al., 2020). With regard to model-based gait-generation methods for uphill and downhill terrain, Kuo (2007) simulated human gait using an inverted pendulum, which provided a circular trajectory for the COM rather than a horizontal trajectory. He found that a horizontal COM trajectory consumed more muscle energy. Massah et al. (2012) utilized a 3D LIPM and the concept of zero moment point (ZMP). They developed a trajectory planner using the semi-elliptical motion equations of an NAO humanoid robot and simulated walking on various sloped terrains using the Webots platform.

In bipedal robot motion control based on the LIPM, the COM, ZMP, and capture point (CP) are crucial factors for achieving stable walking. Addressing the issue of implementing synchronized stabilization control schemes for ZMP and COM, Choi et al. (2007) introduced a kinematic decomposition method for the COM Jacobian matrix, including embedded desired task motion. Hof (2008) independently introduced the CP concept, which defined the position where a bipedal robot can step on the ground to achieve complete stoppage, thereby providing a simple walking balance-control method. Building upon the CP concept, Englsberger et al. (2011) developed a trajectory generator and feedback controller for bipedal robots. Joe and Oh (2018) proposed an online walking-pattern-generation algorithm based on footprint adjustment, enabling bipedal robots to effectively restore walking balance after external disturbances.

Yamamotoa et al. (2020) briefly surveyed the centroidal dynamics and the zero-moment point based on the LIPM and some of its variations; they reviewed many representative standing and walking control techniques based on the LIPM, and also discussed the concept of capturability. Recently, Park et al. (2022) proposed a new stability criterion for bipedal walking systems based on the LIPM, in which the dynamic relationship between the COM and the ZMP was dealt with. Furthermore, the adaptive-network-based fuzzy inference system (ANFIS) was combined with the double deep Q-network (DDQN) to realize a fuzzy DDQN (FDDQN), such that a bipedal robot could generate an LIPM-based gait pattern in real time. This not only allowed the bipedal robot to correct its gait pattern instantly but also improved its stability (Li et al., 2022).

Kajita et al. (2014) ensured the simplicity and flexibility of classical gait-planning methods, borrowing the idea of "preview controllers" that optimize current decisions based on future information to optimize the inevitable foot-placement deviations in classical gait-planning methods. Based on the LIPM, we proposed a closed-loop feedback-control method for bipedal robot COM trajectory planning and resistance to external force disturbances based on CP-ZMP-COM dynamics. The method is based on our analysis of the

✉ Chunbiao GAN, cb_gan@zju.edu.cn

Chunbiao GAN, https://orcid.org/0000-0002-6597-5605

Received Feb. 2, 2024; Revision accepted June 5, 2024;
Crosschecked Mar. 28, 2025

COM motion trajectories in the sagittal and coronal planes.

2 COM trajectory planning based on CP-ZMP-COM dynamics

As shown in Fig. 1a, the LIPM maintains the COM of a bipedal robot moving on a horizontal plane with a height of z_0, using a scalable and massless leg with its pivot located at the robot's ZMP. The *oxyz* is the the world coordinate system $\{W\}$, $o_a x_a y_a z_a$ is the ankle joint coordinate system $\{A\}$, and $o_b x_b y_b$ is the COM plane frame with its *x*- and *y*-direction aligned to $\{B\}$. In the LIPM, the equations of motion for the robot's COM are linear and decoupled, and the dynamical analysis can be equivalently and independently used for the two components *x* and *y* of the robot. Fig. 1b presents the decoupled model of the 3D LIPM in the *xz* plane, where the position of the robot's COM is expressed as $\boldsymbol{p}_c=[\boldsymbol{x}_{com}, z_0]^T$, and the position of COM

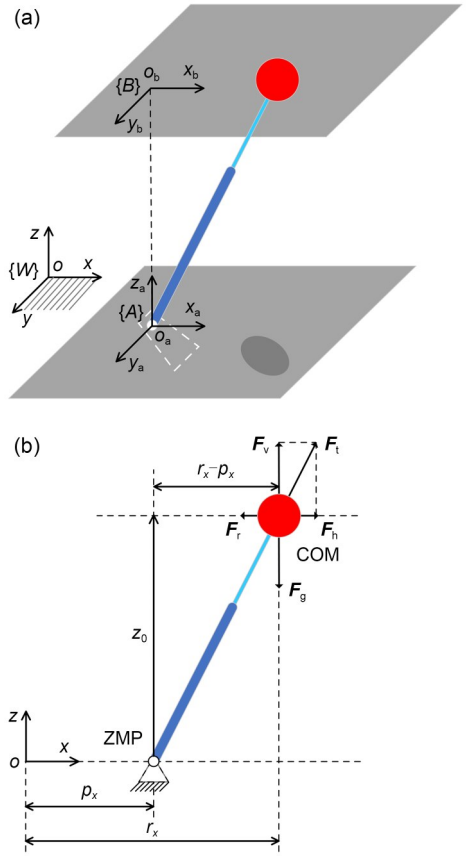

Fig. 1 LIPM for the bipedal robot: (a) 3D model; (b) decoupled model in the *xz* plane

in the *xy* plane is $\boldsymbol{x}_{com}=[r_x, r_y]$, where r_x and r_y represent the COM coordinates along the *x*- and *y*-direction, respectively; the pivot (i.e., ZMP point) position is $\boldsymbol{p}_a=[p_x, p_y]^T$, where p_x and p_y represent the ZMP coordinates along the *x*- and *y*-direction, respectively; the ground reaction force $\boldsymbol{F}_t$ acts through the pivot and COM; $\boldsymbol{F}_v$ and $\boldsymbol{F}_h$ are its components in the *z* and *x* directions, respectively; $\boldsymbol{F}_r$ is the external force acting on the COM in the *x* direction; $\boldsymbol{F}_g$ is the gravity. Based on Newton's theorem and the relationship $|\boldsymbol{F}_h|/|\boldsymbol{F}_v|=|\boldsymbol{F}_r|/|\boldsymbol{F}_g|=(m\ddot{x}_{com})/(mg)=(x_{com}-p_x)/z_0$, where m is the mass of whole robot and g is the gravity constant, the dynamic model of the bipedal robot's CP-ZMP-COM can be established as follows:

$$\dot{\boldsymbol{\theta}}=\begin{bmatrix}-\omega_0 & \omega_0\\ 0 & \omega_0\end{bmatrix}\boldsymbol{\theta}+\begin{bmatrix}0\\ -\omega_0\end{bmatrix}\boldsymbol{p}_a, \tag{1}$$

where $\omega_0=\sqrt{g/z_0}$ is the natural frequency of LIPM; $\boldsymbol{\theta}=[\boldsymbol{x}_{com}, \boldsymbol{\xi}]^T$ is the state variable of this state-space equation; $\boldsymbol{\xi}$ is the CP position in the *xy* plane, and $\boldsymbol{\xi}=[\xi_x, \xi_y]=\boldsymbol{x}_{com}+\dot{\boldsymbol{x}}_{com}/\omega_0$, where ξ_x and ξ_y represent the CP coordinates along the *x*- and *y*-direction, respectively. The detailed derivation for Eq. (1) is presented in Section S1 of the electronic supplementary materials (ESM).

The COM trajectory planning method for the bipedal robot was based on CP-ZMP-COM dynamics and can be briefly outlined as follows: by utilizing the ZMP-CP dynamics $\dot{\boldsymbol{\xi}}=\omega_0(\boldsymbol{\xi}-\boldsymbol{p}_a)$, the CP-COM dynamics $\dot{\boldsymbol{x}}_{com}=-\omega_0(\boldsymbol{x}_{com}-\boldsymbol{\xi})$ automatically track the CP. By adjusting the robot's foot placement to control the COM trajectory, as represented by the ZMP-COM dynamics, the robot's COM trajectory can be planned. The kinematic relationship among ZMP, CP, and COM is shown in Fig. 2, where $\boldsymbol{\xi}_0$ and $\boldsymbol{\xi}_e$ are the expected initial and final position of the CP trajectory; $\boldsymbol{x}_{com,0}$ and $\boldsymbol{x}_{com,e}$ are the expected initial and final position of the COM trajectory; the specific steps are also listed in Section S1 of the ESM.

It should be noted that due to the discrepancy between the real robot dynamics and the simplified inverted pendulum dynamics (Fig. 6 in Section 4), using this controller will result in a non-constant ZMP (Fig. 7). However, it still ensures that the robot's ZMP remains within a feasible range for walking continuously without falling when there is no external

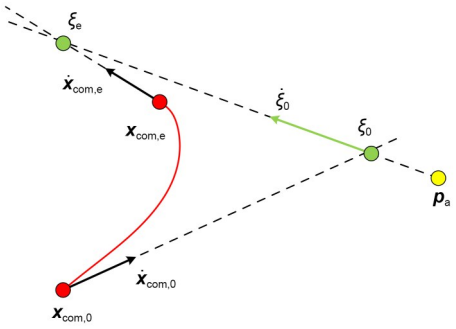

Fig. 2 Kinematic relationship among ZMP, CP, and COM. The path of COM is represented by the red curve. References to color refer to the online version of this figure

disturbance imposed on the robot (the screenshots shown in Fig. 7).

3 Anti-disturbance feedback compensation control

During walking, adults exhibit a swaying motion of their COMs in the sagittal plane, resembling that of an inverted pendulum, as they dynamically adjust their step lengths. This allows for either short and quick steps or long and slow steps, while maintaining constant COM walking speed. Therefore, coordinating the foot placement of the robot in both the sagittal and coronal planes was crucial to counteracting external disturbances.

Inspired by this, further characterization of the robot's gait parameters during walking was required. As shown in Fig. 3, the LIPM was placed in the ankle joint coordinate system $\{A\}$ of the stance foot (i.e., ZMP point, as shown in Fig. 1a). In ideal conditions, the undisturbed trajectory of the robot's COM serves as the nominal gait reference trajectory, based on which the gait parameters are explicitly defined to avoid confusion.

As shown in Fig. 3, the reference trajectory of the bipedal robotic walking, which switches supporting

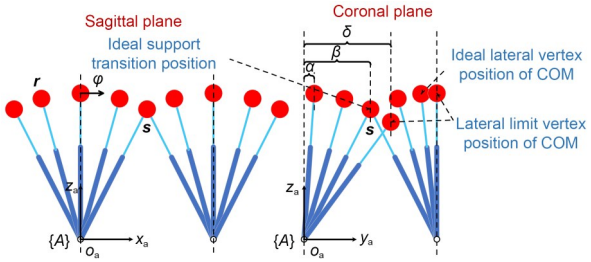

Fig. 3 Gait parameters in sagittal and coronal planes of the bipedal robot during walking process

legs, takes its COM state $\boldsymbol{r}=[r_x,\ r_y,\ r_z]^{\mathrm{T}}$ as the ideal characteristic gait, where r_z is the z-coordinate of the COM, depending solely on its walking velocity $\boldsymbol{v}$ and four additional gait parameters (α, β, δ, and φ). α represents the distance between the origin of the ankle joint coordinate system $\{A\}$ and the COM in the y-direction (lateral) when the COM is at the coronal-plane vertex position (at which time the velocity $\dot{c}_y$ of COM in the y-direction is 0); β represents the distance in the y-direction between the COM and the ankle joint coordinate system when exchanging supporting feet; δ represents the distance between COM and the origin of the ankle joint coordinate system in the y-direction (in the sagittal plane) under the limit state of exchanging support, at which time the velocity $\dot{c}_y$ of COM in the y-direction is at its maximum of $v_y^{\max}$; φ represents the magnitude of COM velocity in the x-direction $\dot{c}_x$ when COM is at the vertex position of the sagittal plane (at which time $v_x^{\max}$ is the maximum velocity of COM). Additionally, when the robot's COM is at the position defined by parameter α, the lateral component of the COM velocity is zero. As long as α is greater than zero, the COM will tend towards the direction of the next foothold and ensure that the support exchange position is reached within the ranges of β and δ.

Let $\boldsymbol{v}=[v_x,\ v_y]^{\mathrm{T}}$ denote the desired walking-velocity input vector, where v_x and v_y represent the reference walking speed in the forward and lateral directions, respectively. According to the COM dynamics (Eq. (S2) in Section S1 of the ESM), the ideal COM state during support exchange is given by $\boldsymbol{s}=[s_x,\ \dot{s}_x,\ s_y,\ \dot{s}_y]^{\mathrm{T}}$, where

$$s_y=\begin{cases}\lambda\zeta, & \text{if } \lambda=\operatorname{sgn}(v_y),\\ \lambda\beta, & \text{else},\end{cases} \tag{2a}$$

$$\dot{s}_y=\lambda C\sqrt{s_y^2-\alpha^2}, \tag{2b}$$

$$s_x=\frac{\varphi v_x}{Cv_x^{\max}}\sinh(C\tau), \tag{2c}$$

$$\dot{s}_x=\frac{\varphi v_x}{v_x^{\max}}\cosh(C\tau), \tag{2d}$$

$$\zeta=\beta+v_y(\delta-\beta)/v_y^{\max}, \tag{2e}$$

$$\tau=\frac{1}{C}\ln\left(\frac{\zeta}{\alpha}+\sqrt{\frac{\zeta^2}{\alpha^2}-1}\right). \tag{2f}$$

In Eq. (2a), s_y denotes the COM position in y-direction; ζ denotes the lateral support-swapping position required when the robot needs lateral walking

speed; $\lambda\in\{-1, 1\}$ represents the left-right sign of the assumed supporting leg; in Eq. (2c), s_x denotes the COM position in x-direction; τ stands for the transition time of COM from the vertex to the support-swapping position; C is the parameter reflecting the gravitational influence on the point-mass trajectory (Pratt et al., 2006). The COM state $\boldsymbol{s}$ at this ideal support-swapping position defines the goal of the controller, aiming to adjust the foothold to achieve this goal at the end of the next step.

Based on the above analysis, the specific steps for the feedback compensation control method are as follows:

Step 1 Input the initial desired walking velocity vector $\boldsymbol{v}_0$, and calculate the ideal COM state trajectory $\boldsymbol{s}=[s_x, \dot{s}_x, s_y, \dot{s}_y]^{\mathrm{T}}$ using COM dynamics (Eq. (S2) in Section S1 of the ESM), and then proceed to Step 2.

Step 2 Based on the actual COM state $\boldsymbol{c}=[c_x, \dot{c}_x, c_y, \dot{c}_y]^{\mathrm{T}}$ in the current ankle joint coordinate system of the biped robot and the ideal COM state $\boldsymbol{s}=[s_x, \dot{s}_x, s_y, \dot{s}_y]^{\mathrm{T}}$ during support switching, calculate the following five compensation parameters, i.e., lateral ZMP compensation y_{offset}, support-switching time interval dT, lateral step width L_y, forward ZMP compensation x_{offset}, and forward step length L_x (which are listed in Section S1 of the ESM), and then proceed to Step 3.

Step 3 Substitute the results of Step 2 into the CP controller: $p_x=\dfrac{\xi_{x,\mathrm{d}}-\mathrm{e}^{\omega_0 \mathrm{d}T}\xi_x}{1-\mathrm{e}^{\omega_0 \mathrm{d}T}}=\dfrac{1}{1-b}\xi_{x,\mathrm{d}}-\dfrac{b}{1-b}\xi_x$ (Eq. (S9) in Section S1 of the ESM), where p_x is the ZMP position in x-direction; $\xi_{x,\mathrm{d}}$ is desired destination of CP in x-direction and $b=\mathrm{e}^{\omega_0 \mathrm{d}T}$. Update and record the coordinates of the support leg and the ideal COM state, and then proceed to Step 4.

Step 4 Based on the results recorded in Step 3, input the reference trajectories of each joint obtained from inverse kinematics calculations into the prototype servos to achieve walking control of the prototype. Update and record the coordinates of the support leg and the actual COM state of the physical prototype using joint encoders and an inertial measurement unit (IMU), and then proceed to Step 5.

Step 5 Compare and analyze the errors between the coordinates of the support leg and the COM state under ideal conditions, and the coordinates of the support leg and the COM state of the actual physical prototype. Return to Step 2.

The algorithm flowchart for the feedback compensation control method is given in Fig. 4.

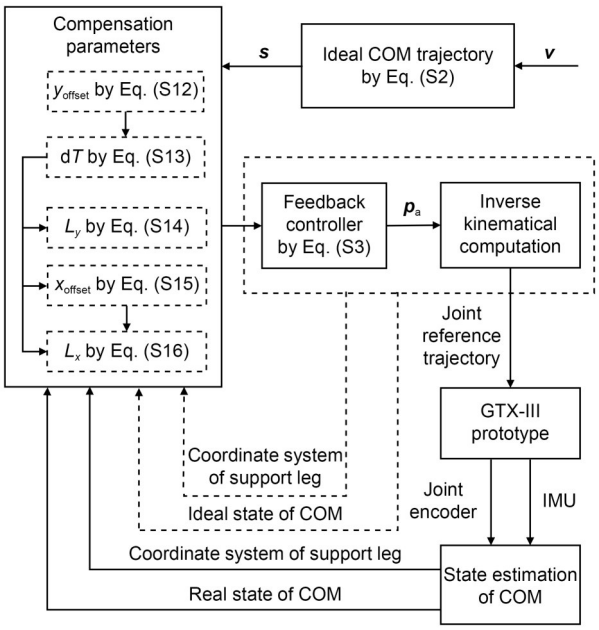

Fig. 4 Algorithm flowchart for the feedback compensation control method

4 Simulation and experimental validation

As shown in Fig. 5a, the bipedal robot considered in this study is the GTX-III prototype, with a total mass and upright COM height of 4.8 kg and 25.6 cm, respectively. Utilizing the 3D simulation model of GTX-III built in Simulink (Fig. 5b), lateral walking, diagonal walking, and turning in place in ideal environments without disturbances or modeling errors were accomplished based on the COM trajectory-planning method proposed in Section 2. Typical lateral walking is illustrated in Fig. 6 and lateral walking experimental video screenshots are shown in Fig. 7.

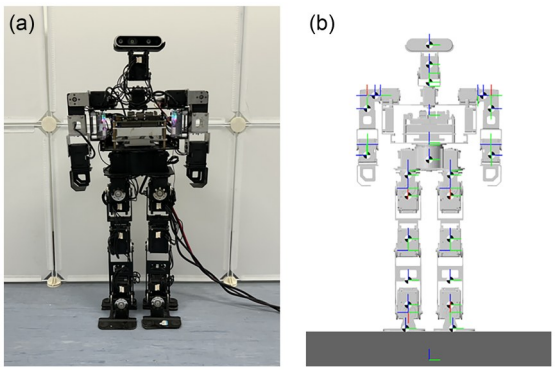

Fig. 5 Miniature bipedal robot GTX-III: (a) physical prototype; (b) Simulink simulation model

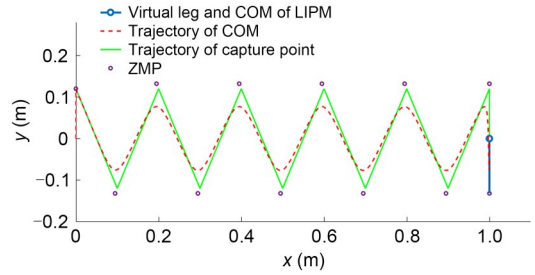

Fig. 6 Lateral walking simulation results based on the COM trajectory-planning method with a lateral step width of 0.1 m and ideal walking cycle of 0.8 s

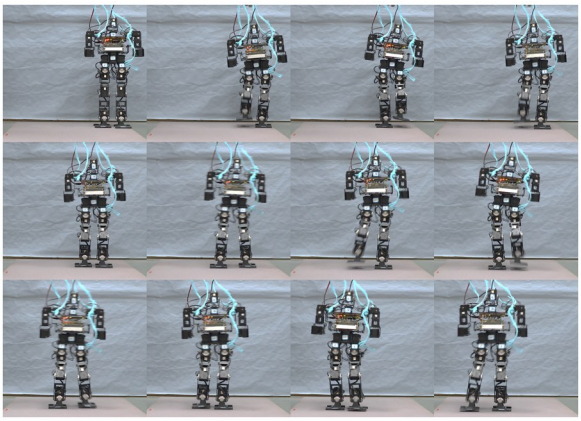

Fig. 7 Screenshots from lateral experiments based on the COM trajectory-planning method

The following assumptions were made regarding disturbances during the robot's walking process: 1) external force disturbances were assumed to be impulse forces directly acting through the COM of the robot in three directions (generated by calling MATLAB's random number seed) with amplitudes varying between −10 N and 10 N; 2) disturbances occurred only once within a single complete gait cycle. The robot was set to walk along a straight line with an ideal support-switching interval of 0.8 s and an initial step length of 0.05 m. Simulation results are shown in Fig. 8. The randomly generated impulse forces acting through the COM of the robot at the beginning of each complete gait cycle after three complete gait cycles, i.e., 4.8 s later. Despite the presence of external force disturbances (random impulse forces varying between −10 N and 10 N), the designed disturbance-resistant control method based on bidirectional coordination promptly adjusted the foothold position to counteract the effects of external force disturbances. Although the direction of disturbance was random, similar to the characteristics of LIPM motion described in Section 2, the robot

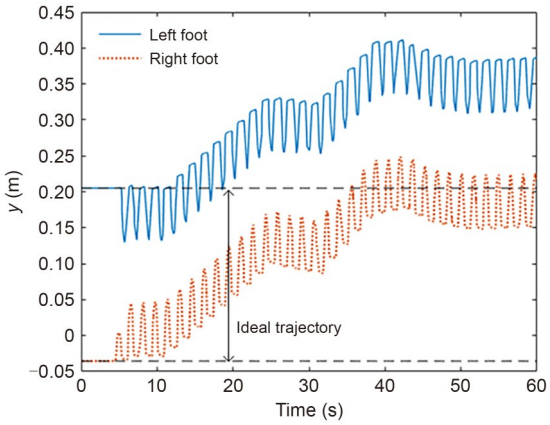

Fig. 8 Simulation results of lateral walking with resistance to random impulse disturbance based on foot placement and COM state feedback compensation

had greater freedom in forward motion. Therefore, deviations from the planned trajectory in the forward direction were smaller. However, the robot's robustness to external force disturbances was weaker in the lateral direction, necessitating adaptive adjustments in step width to accommodate external force disturbances. These adjustments allowed the COM to return to the center between the two legs through the next support switch, thus maintaining balance.

Building upon the aforementioned simulation analysis, we further conducted impact resistance tests on the bipedal robot prototype GTX-III. Screenshots from experimental video of the disturbance-resistant walking control are shown in Fig. 9. As depicted in Fig. 9, the

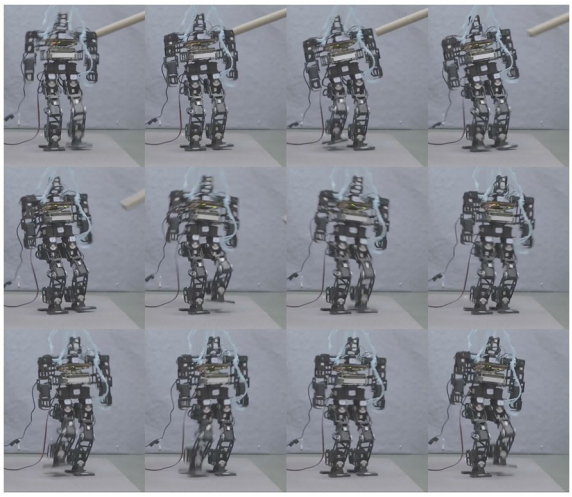

Fig. 9 Screenshots from experimental video of lateral walking with resistance to random impulse disturbances based on foot placement and COM state feedback compensation

disturbance-resistant control strategy based on foothold-position adjustments maintained the robot's balance even in the presence of thrust disturbances. In contrast, using the COM trajectory-planning method proposed earlier resulted in imbalance under external force disturbances (omitted for brevity). Additionally, this disturbance-resistant control method effectively counteracted random external force disturbances with only a single IMU, without relying on pressure sensors on the foot sole or visual sensors. This not only provided space for subsequent multisource sensor-information fusion but also confirmed the strong robustness of the proposed disturbance-resistant control method based on foothold adjustments.

5 Conclusions

In this study, we first analyzed the sagittal- and coronal-plane motion during robotic walking using the LIPM, and established the CP-ZMP-COM dynamic model for it. Based on this, we proposed an improved COM trajectory-planning method to achieve flexible robotic walking on flat terrain. When the robot is subjected to external force disturbances, a disturbance-resistant control strategy based on foothold and COM position adjustments can be used: when the COM reaches the support-leg swap position roughly centered in the step width, the expected touchdown time is determined by the lateral COM trajectory. By selecting appropriate lateral step widths, the COM can swing back and transition to another direction; for the highly flexible forward direction, suitable step lengths are chosen to adapt to the variations in step time while maintaining the desired forward velocity; finally, the foothold is compensated for to achieve closed-loop feedback control.

We validated the effectiveness of the COM trajectory-planning method and disturbance-resistant control strategy through experiments testing flexible walking and resistance to random impulse external force disturbances of the GTX-III prototype and its simulation model, including lateral walking, diagonal walking, and turning in place.

This work implements and experimentally validates the proposed method on the GTX-III robot, achieving closed-loop control with only a single IMU sensor, thereby eliminating the traditional reliance on foot pressure or vision sensors. By leveraging the relationship between the CP and ZMP, the control strategy adaptively selects appropriate step lengths in the highly flexible forward direction to accommodate variations in step timing while maintaining the desired forward velocity under external disturbances. In general, the proposed method realizes closed-loop feedback control for disturbance rejection through foothold position compensation.

Acknowledgments

This work is supported by the National Natural Science Foundation of China (No. 12332023) and the Zhejiang Provincial Natural Science Foundation of China (No. LY23E050010).

Author contributions

Chunbiao GAN: oversight and leadership responsibility for this research activity planning and execution. Zijing LI: original draft including preparation and creation of the published work. Yimin GE: design of methodology and application of mathematical and computational techniques. Mengyue LU: partially process of the corresponding data.

Conflict of interest

Chunbiao GAN, Zijing LI, Yimin GE, and Mengyue LU declare that they have no conflict of interest.

References

Choi Y, Kim D, Oh Y, et al., 2007. Posture/walking control for humanoid robot based on kinematic resolution of CoM Jacobian with embedded motion. *IEEE Transactions on Robotics*, 23(6):1285-1293. https://doi.org/10.1109/TRO.2007.904907

Englsberger J, Ott C, Roa MA, et al., 2011. Bipedal walking control based on capture point dynamics. IEEE/RSJ International Conference on Intelligent Robots and Systems, p.4420-4427. https://doi.org/10.1109/IROS.2011.6094435

Englsberger J, Ott C, Albu-Schäffer A, 2015. Three-dimensional bipedal walking control based on divergent component of motion. *IEEE Transactions on Robotics*, 31(2):355-368. https://doi.org/10.1109/TRO.2015.2405592

Hof AL, 2008. The 'extrapolated center of mass' concept suggests a simple control of balance in walking. *Human Movement Science*, 27(1):112-125. https://doi.org/10.1016/j.humov.2007.08.003

Joe HM, Oh JH, 2018. Balance recovery through model predictive control based on capture point dynamics for biped walking robot. *Robotics and Autonomous Systems*, 105: 1-10. https://doi.org/10.1016/j.robot.2018.03.004

Kajita S, Hirukawa H, Harada K, et al., 2014. Introduction to Humanoid Robotics. Springer, Berlin Heidelberg, Germany. https://doi.org/10.1007/978-3-642-54536-8

Kuo AD, 2007. The six determinants of gait and the inverted pendulum analogy: a dynamic walking perspective. *Human Movement Science*, 26(4):617-656. https://doi.org/10.1016/j.humov.2007.04.003

Li THS, Kuo PH, Chen LH, et al., 2022. Fuzzy double deep Q-network-based gait pattern controller for humanoid robots. *IEEE Transactions on Fuzzy Systems*, 30(1):147-161. https://doi.org/10.1109/TFUZZ.2020.3033141

Massah BA, Sharifi KA, Salehinia Y, et al., 2012. An open loop walking on different slopes for NAO humanoid robot. *Procedia Engineering*, 41:296-304. https://doi.org/10.1016/j.proeng.2012.07.176

Owaki D, Koyama M, Yamaguchi S, et al., 2010. A two-dimensional passive dynamic running biped with knees. IEEE International Conference on Robotics and Automation, p.5237-5242. https://doi.org/10.1109/ROBOT.2010.5509166

Park HY, Kim JH, Yamamoto K, 2022. A new stability framework for trajectory tracking control of biped walking robots. *IEEE Transactions on Industrial Informatics*, 18(10):6767-6777. https://doi.org/10.1109/TII.2021.3139909

Pratt J, Carff J, Drakunov S, et al., 2006. Capture point: a step toward humanoid push recovery. The 6th IEEE-RAS International Conference on Humanoid Robots, p.200-207. https://doi.org/10.1109/ichr.2006.321385

Xie HL, Zhao XF, Sun QC, et al., 2020. A new virtual-real gravity compensated inverted pendulum model and ADAMS simulation for biped robot with heterogeneous legs. *Journal of Mechanical Science and Technology*, 34(1):401-412. https://doi.org/10.1007/s12206-019-1239-4

Yamamoto K, Kamioka T, Sugihara T, 2020. Survey on model-based biped motion control for humanoid robots. *Advanced Robotics*, 34(21-22):1353-1369. https://doi.org/10.1080/01691864.2020.1837670

Electronic supplementary materials

Section S1, Eqs. (S1)–(S16)